In this note we summarize the consequences for the measurement of low mass vector mesons, if during first operation of PHENIX only 1/2 or 1/4 of the readout electronics will be available. As a reference we use the yields expected for a complete setup.

The parameters chosen for all simulations are given in appendix 1. The relative abundances of various meson species at freeze-out are scaled from pp interactions. We assume isotropic production in azimuthal direction, flat rapidity distribution around $y_{cm} = 0$ and mt-scaling. For the mt-slope we have chosen 220 MeV, consistent with RQMD predictions. The rate estimates are based on a luminosity of 20 μb^{-1}, expected to be reached at the end of the first physics run. We consider one 1/4 of luminosity as intermediate step, referred to as rates for Day-1.

We have studied the decays of the vector mesons ρ, ω, ϕ and J/ψ to e^+e^- as well as $\phi \to K^+K^-$. Besides these decays we have also simulated background. For $\phi \to K^+K^-$ inclusive kaon production rates are used. Background electron pairs arise from photon conversions, π° and η Dalitz decays. Tracks from photon conversion in the beam pipe and MVD conversions are considered indistinguishable from vertex tracks all, other conversions are assumed to be rejectable. The background contribution of open charm decays was neglected. This together with the assumed perfect electron identification creates a softer mass distribution, resulting in an optimistic background at the ϕ mass.

To avoid tracking particles through a full GEANT simulation and subsequent analysis chain, we have developed a filter which parameterizes the PHENIX central detector acceptance. Based on the 3 momentum it returns whether or not a particle would have traversed either of the two drift chambers and has hit PC3 on the same side. Effectively this corresponds to a 200 MeV lower momentum cut. In polar angle the acceptance is limited to 70 to 110 degree. Details on the filter can be found in appendix 2. We assume perfect particle identification and track reconstruction. The momentum resolution was set to $\sigma_p/p = 0.005 * \sqrt{1+p^2}$ in accordance with the CDR.

Besides two completed arms we have studied various scenarios of two partially equipped arms as well as one arm full or half equipped. Detailed comparisons of different geometrical placement of electronics can be found in appendix 2. Different placements give mostly similar results, however, on a 30% level the acceptance can be optimized. Note that the result will depend on the decay chosen to optimize the geometry. The acceptance was folded with the pt-distribution and the expected luminosity for full year one running.

First we consider $\phi \to K^+K^-$, which due to its large branching ratio can be measured with low luminosity on Day-1, even with partial acceptance coverage. All details can be found in appendix 3. The low Q-value of the decay together with the momentum cut-off at 200 MeV prohibits the measurement of ϕ with pt smaller than 400 MeV. At this pt the opening angle is small enough that K^+ and K^- will be accepted in the same arm.

The rate estimates are for one arm equipped with half the electronics. At Day-1, we expect about 30K ϕ's of which 1/3 is from central events. The signal-to-background is about 6% in central events, leading to an error in the cross section measurement of about 4% (Figure 1 of the appendix) assuming no systematic errors. At the end of year 1 we will have enough statistics to make several bins in centrality and mt. This will allow us to make a measurement of the inverse slope parameter at various centralities to about 15%, and to study yields and line shape as a function of centrality.

Vector meson decays to electron pairs can not be measured in the above detector configuration. All rate estimates have been done for more complete setups and the luminosity reached at the end of the first year, for details see appendix 4. The signal to background ratios were evaluated for a 1.64 sigma (width folded with resolution) region around each vector mesons, which contains 90% of the signal.

For 120 M minimum bias events we expect 5100 ω's, 2300 ϕ's and 2800 J/ψ's within the full PHENIX central detector acceptance. Taking into account the signal to background ratios these yields allow cross section measurements with 6%, 3.5% and 2% statistical error for ω, ϕ and J/ψ, respectively. For central events errors will increase to 15%, 8% and 3.5%. Finite pair reconstruction efficiency will increase the error further by $1/\sqrt{\epsilon_{pair}}$. Even for a pessimistic pair reconstruction efficiency of $\sim$ 25% the errors would only double, still allowing a reasonable measurement of ϕ and J/ψ.

If only one arm is equipped with electronics the rates are reduce dramatically. We find 650 ω's, 135 ϕ's and no J/ψ's, where the ω's are restricted to pt>500 MeV and the ϕ's to pt>1 GeV. The statistics will be insufficient for any measurement.

However, distributing the same amount of electronics over both arms restores a significant acceptance for all pt. Compared to the full acceptance the rates are reduced by approximately a factor of 4 resulting in 1100 ω's 600 ϕ's and 650 J/ψ's from the minimum bias sample. The expected statistical errors will increase by only a factor of 2, still allowing a reasonable measurement of ϕ and $J\psi$ cross sections at RHIC.

Appendix 1

Summary of input parameters used for calculations

This is a summary of input parameters used for the calculations done by the Low-Mass Vector Meson working group for this report.

```
Luminosities
        Day-1 5 inverse microbarns -> 3M Central events
        Day 1.5 (i.e. at the end of year 1) 20 inverse microbarns
                -> 12M Central events, 120M min-bias events

For Central events
(dN/dy) for pi0 =500 = pi+ =pi-
We will throw particles in a range y=+-0.5

K+/Pi0= 0.16
rho/pi0 = 0.16
phi/pi0=0.015

K+/pi0=0.15
K-/pi0=0.10

For Min Bias events
(dN/dY) for pi0 =150
  all ratios stay the same as central

Assume Mt scaling - all inverse slope parameters 220 MeV
  (pi,K,rho,omega,phi) and flat in rapidity.
```

Appendix 2 - Acceptance filter

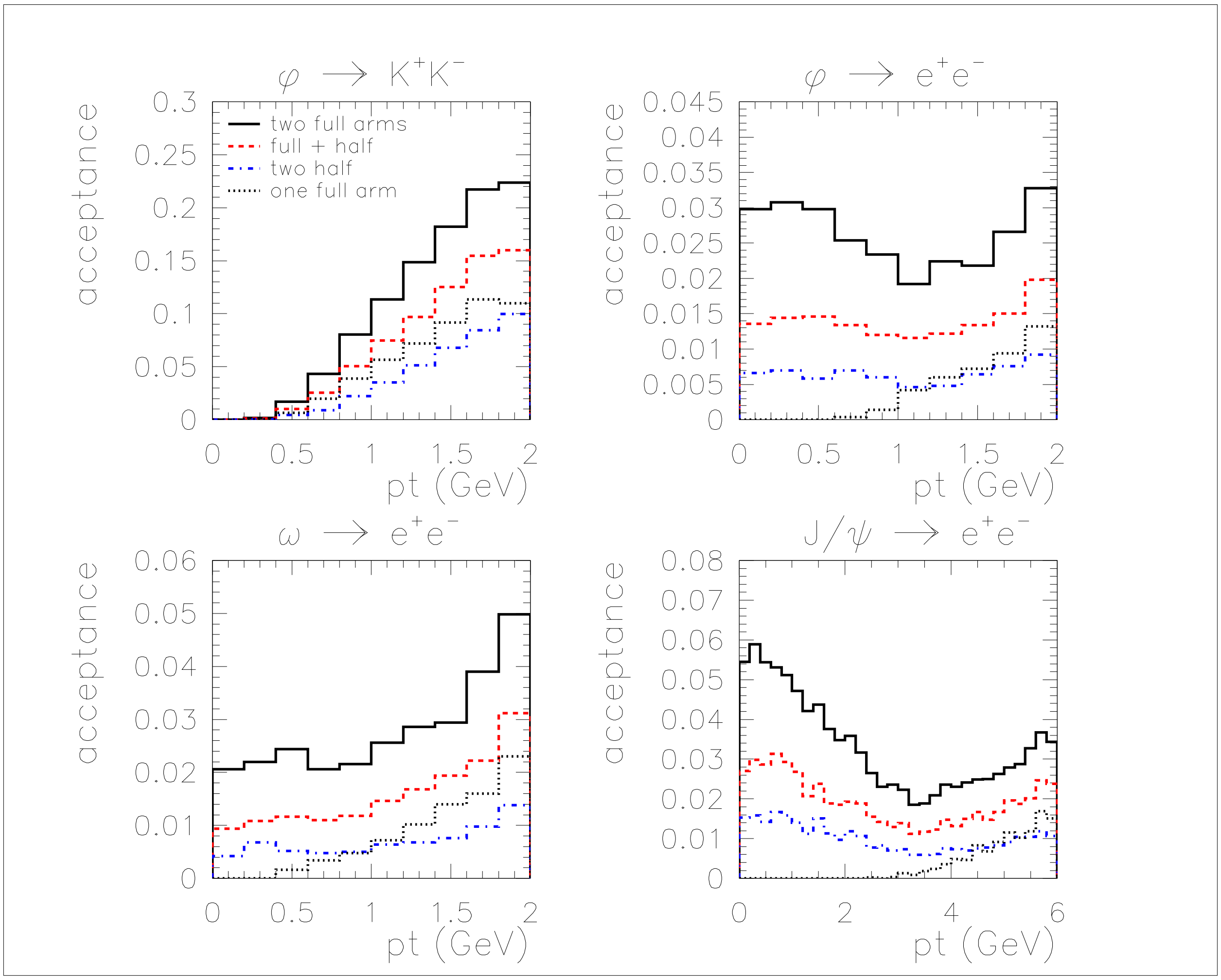

Figure 1: pt acceptance for (a) $\phi \rightarrow K^+K^-$, (b) $\phi \rightarrow e^+e^-$, (c) $\omega \rightarrow e^+e^-$, and (d) $J\psi \rightarrow e^+e^-$

Appendix 3 - Phi to KK study

The simulation for ϕ to KK were done using the acceptance filter described previously. These simulations assume we have used the timing from the EMCal. The TOF resolution is of course much better and will improve these results significantly. Assuming a timing resolution of 300 ps, Kaons can be identified to 1.3 GeV. Kaon decays are also included where it is assumed that the path to the EMcal is a straight line. Including the correct flight path will degrade these results somewhat.

It is important to note for these simulations that we have chosen parameters from RQMD, which gives a somewhat higher slope for the pions and Kaons, then HIJING, which has been used for simulations up till now. (For reference these figures are shown in figures 6 and 7). The impact of this is that the signal-to-background and therefore the statistical significance of all results is somewhat lower in the present studies as compared to those that have been done previously using Hijing.

Two configurations were considered for day 1. Configuration 1 includes a slice of the detector in $\Delta\phi$, using 1/2 of 4 sectors. Configuration 2 includes 2 full sectors of the detector. The major difference between the two configurations is in the pt acceptance. In the cross section for the ϕ there is about a 20 percent difference in the configurations with configuration 1 favoring high pt and configuration 2 favoring low pt. This is reflected in the invariant mass spectrum of the background. However the total acceptance is essentially the same. The conclusion is that either configuration is good for the ϕ measurement on day 1.

Figure 2 shows the pt acceptance of the ϕ for the two difference detector configurations. As mentioned before there is a slight favoring of configuration2 to lower pt- 20-30% at 700 MeV.

Figure 1 shows the invariant mass spectrum at day 1 for the two configurations before and after background subtraction which was done using a polynomial fit to the background around the vicinity of the ϕ. Because of the differences in pt acceptance of the two configurations, the backgrounds are different. Nevertheless, it is clear that either configuration is adequate to measure the ϕ cross section.

Figure 3 shows the inverse slop parameter measurement possible at the end of year 1 (Day 1.5) assuming configuration 2. Errors are statistical only. The inverse slope parameter can be measured to better than 15%.

Appendix 4 - electron pair study

In order to address electron pair physics and the background associated with it, we assume a yield of particles per event as given in Appendix 1. We have simulated π^0, η, ρ, ω, ϕ, and J/Ψ along with photon conversions with the assumption that conversions are primarily due to a γ's from π^0's interacting in the MVD or beam pipe. Conversions, therefore, were implemented by an effective increase in the Dalitz decay branching ratio according to the amount of material in the detector aperture.

Particles are decayed through the PHENIX spectrometer filter for various detector configurations as described in Appendix 2. The momentum resolution is parameterized as $\delta p/p = 5\%\sqrt{(1+p^2)}$ according to the CDR. Shown in Tables 1 and 2 is the expected yield of each particle type as well as the signal to background at that peak for the mesons in question. The signal to background is determined by integrating the yield $\pm 1.64\sigma$, corresponding to 90% of the signal, compared to the background in that same region. Both 12M central and 120M minimum bias events are shown, corresponding to the expected end of year one integrated luminosity. We assume perfect reconstruction efficiency.

The statistical errors for these measurements can be determined assuming that the errors in the background subtraction will be small compared to the statistical errors of the yield in each bin. In this case, the relative error is given by

$$\delta S/S = \sqrt{S+BG}/S^2 \qquad (1)$$

where S is the signal and BG is the background.

Shown in Fig. 10 is the dN/dp_t distribution of ρ, ω, ϕ and J/Ψ expected in the central 10% collisions after the first year of PHENIX running for various detector configurations. Of particular note, the yield of each specie drops consistently by a factor of 4 in the two half-arm scenario over that of two full arms. However, for the single arm configuration, the yield drops dramatically and a p_t cut off equal to the particle mass is introduced due to the 45 degree acceptance opening. In this case, the yield of J/Ψ drops to zero and any low p_t measurements are impossible.

Finally, in Figure 11 is the invariant mass of all accepted pairs for the full PHENIX detector in the first year of running. The distribution is binned in 3 MeV increments and expected statistical error bars are shown. The same figure assuming two half-arms, is shown in Figure 12.

Particle	2 Full Arms	1 Full Arm	1/2 Arm	2*1/2 Arms
ρ	1120 $\pm$ 1178(1/1240)	135 $\pm$ 344 (1/877)	37 $\pm$ 105(1/300)	280 $\pm$ 595 (1/1264)
ω	1709 $\pm$ 277 (1/44)	214 $\pm$ 88 (1/31)	30 $\pm$ 30(1/30)	382 $\pm$ 125 (1/40)
ϕ	776 $\pm$ 68 (1/5)	45 $\pm$ 13 (1/3)	4	201 $\pm$ 35 (1/5)
J/Ψ	945 $\pm$ 31	0	0	319 $\pm$ 18

Table 1: Yields for 12 Million Central Events (Year 1). The errors correspond to statistical errors in the cross section after subtracting the background. The values in parenthesis are the signal to background ratios. See the text for details.

Particle	2 Full Arms	1 Full Arm	1/2 Arm	2*1/2 Arms
ρ	3360 $\pm$ 1139 (1/385)	405 $\pm$ 323 (1/257)	111 $\pm$ 106 (1/100)	840 $\pm$ 542 (1/350)
ω	5127 $\pm$ 295 (1/16)	642 $\pm$ 95 (1/13)	90 $\pm$ 31 (1/10)	1146 $\pm$ 112 (1/10)
ϕ	2328 $\pm$ 68 (1/1)	135 $\pm$ 12 (3/1)	12	603 $\pm$ 35 (1/1)
J/Ψ	2835 $\pm$ 53	0	0	657 $\pm$ 26

Table 2: Yields for 120 Million Minimum Bias Events (Year 1). The errors correspond to statistical errors in the cross section after subtracting the background. The values in parenthesis are the signal to background ratios. See the text for details.

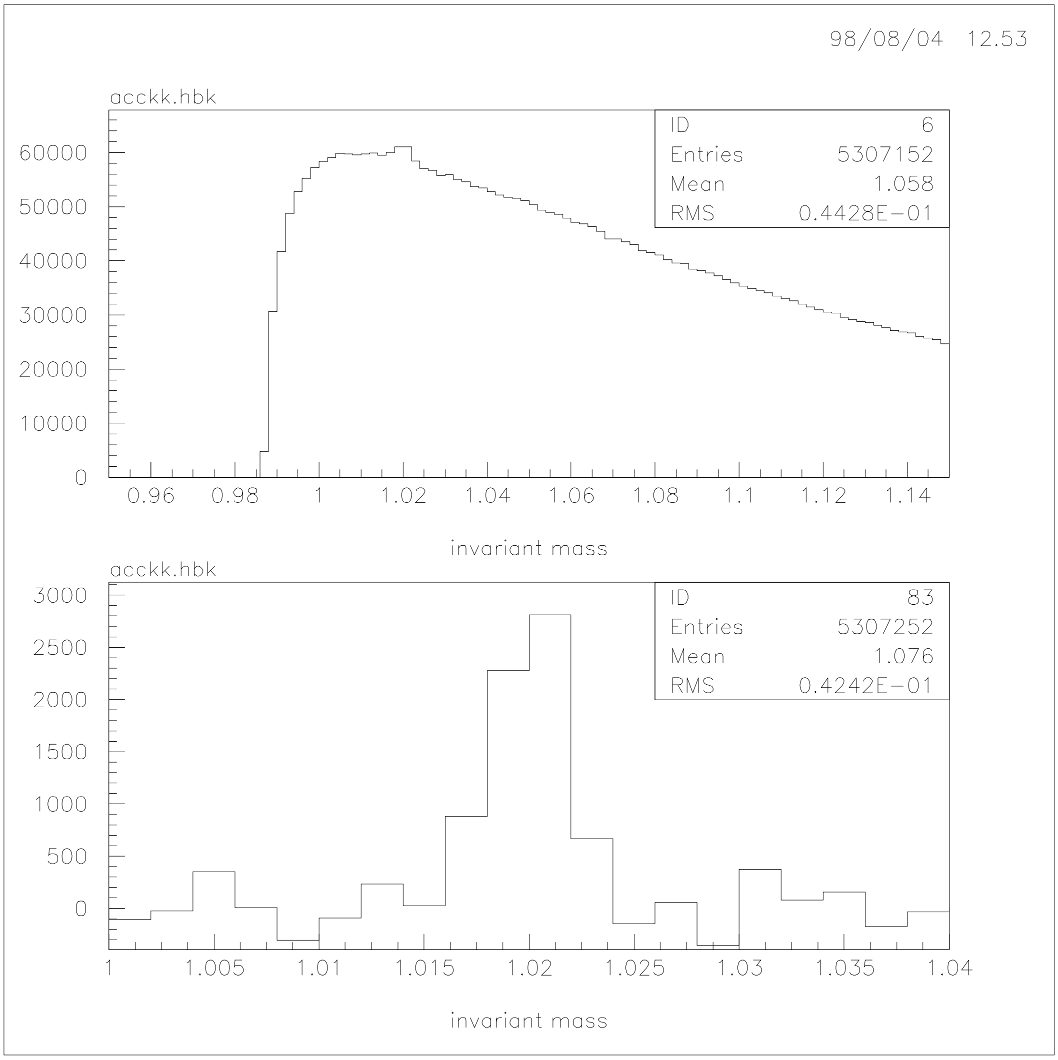

Figure 2: (a) The invariant mass spectrum for K+K- pairs. Cut in $\Delta\phi$ configuration (config 1) (b) Background subtracted

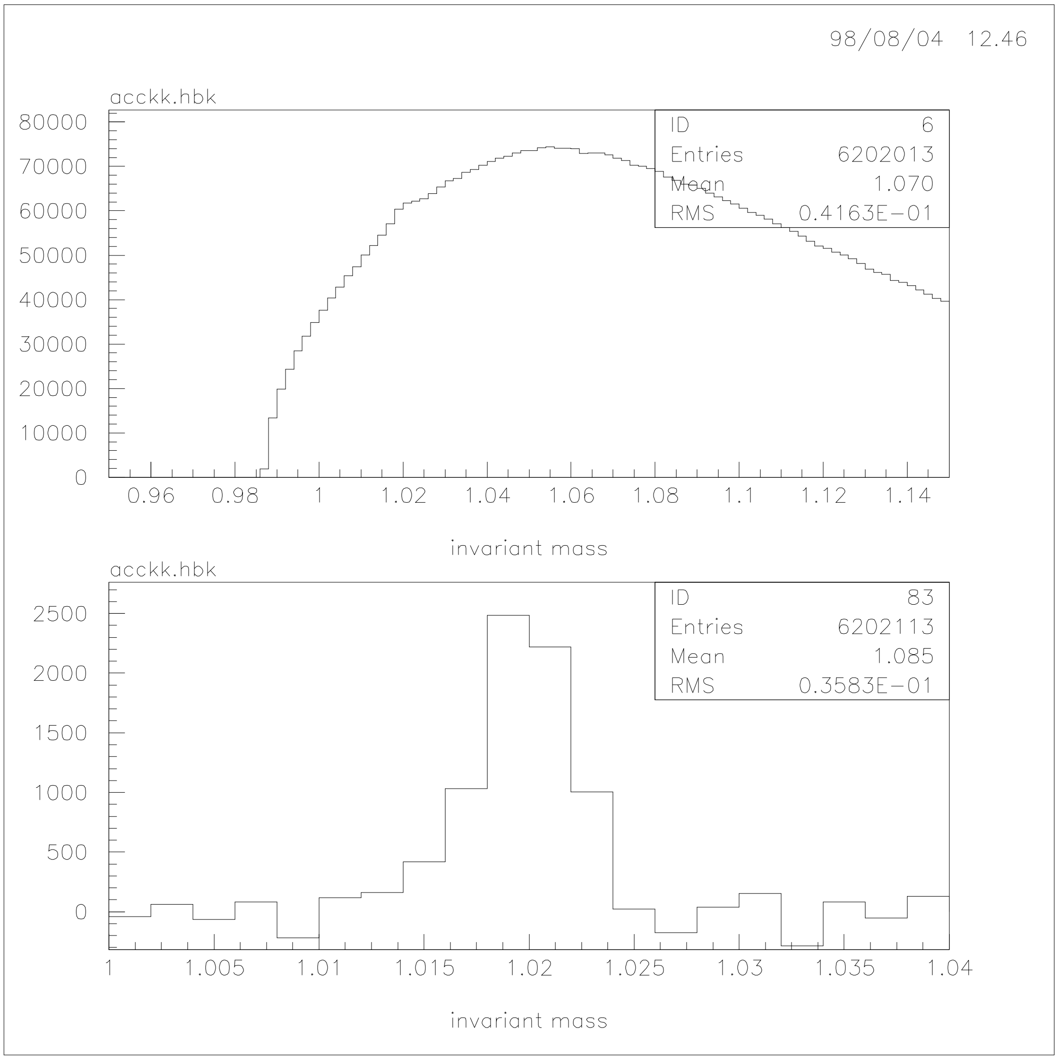

Figure 3: (a) The invariant mass spectrum for K+K- pairs. Configuration using 2 sectors (config 2) (b) Background subtracted

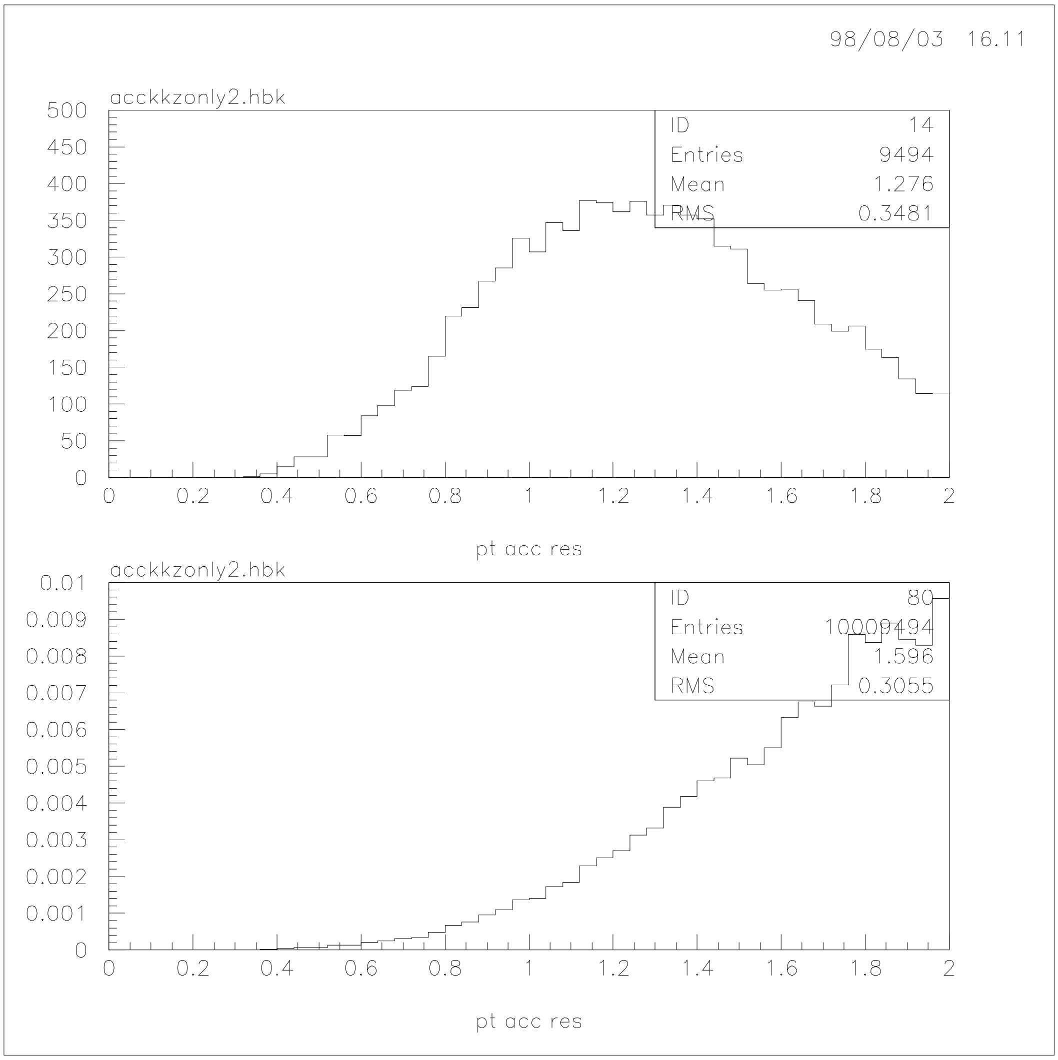

Figure 4: (a) Raw pt spectrum for accepted ϕ's, config 1. (b) Acceptance

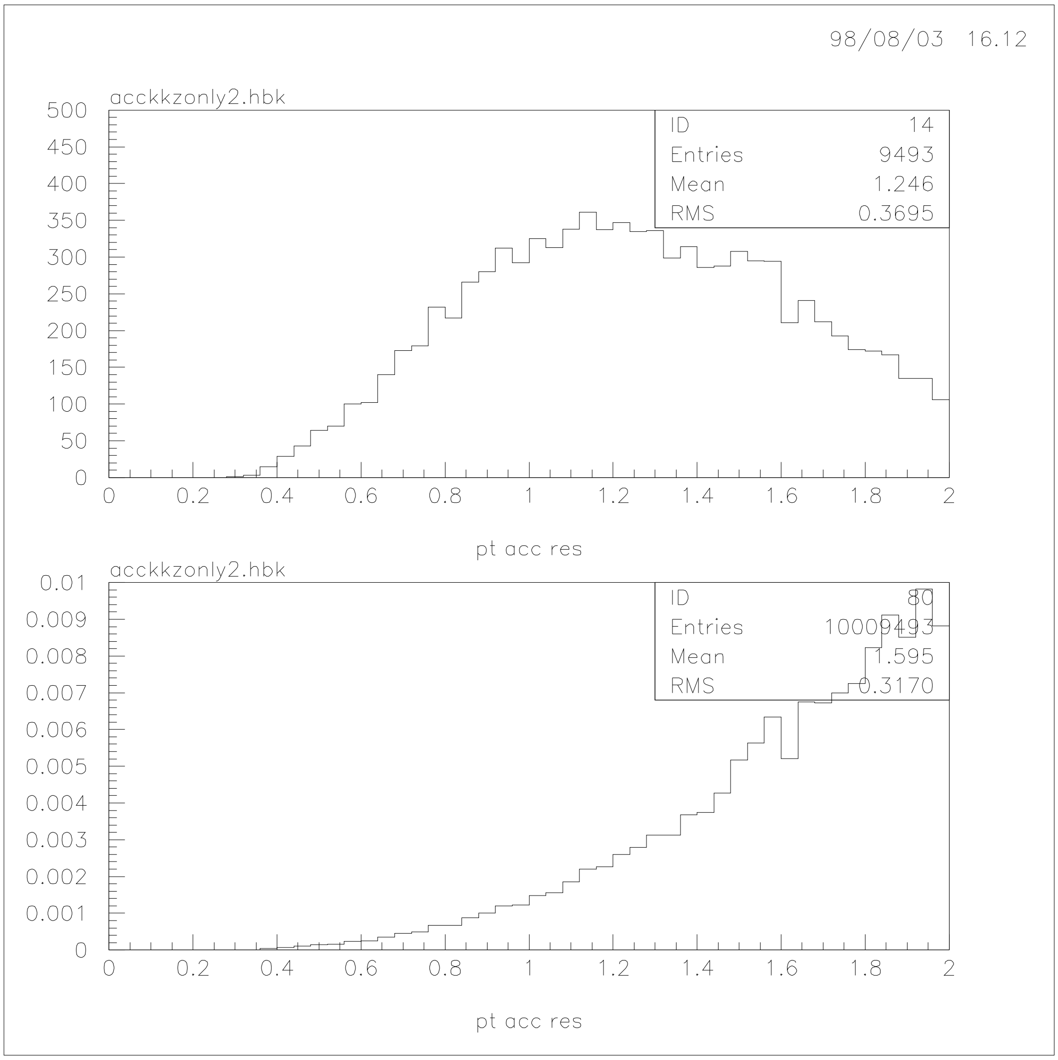

Figure 5: (a) Raw pt spectrum for accepted ϕ's, config. 2. (b) acceptance

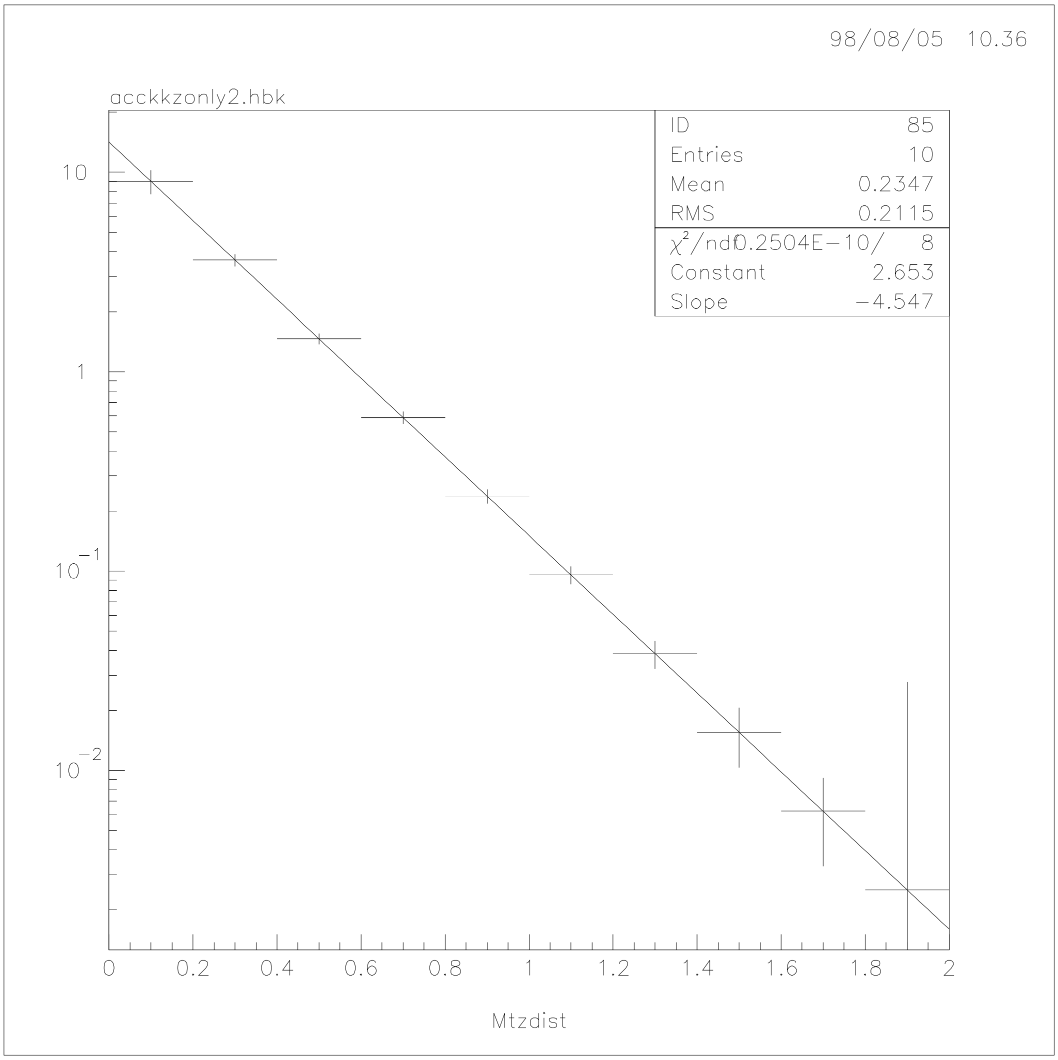

Figure 6: (a) Raw pt spectrum for accepted ϕ's, config. 2. (b) acceptance

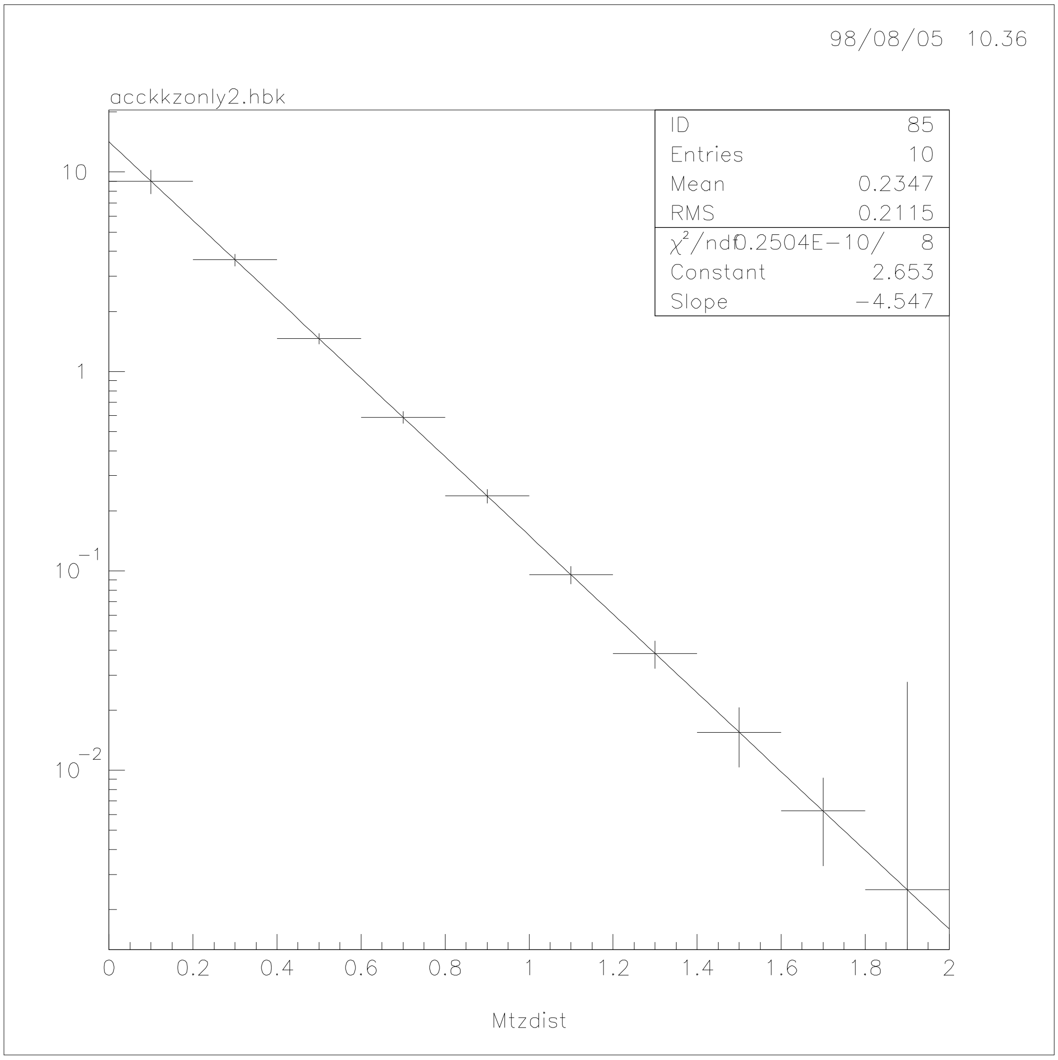

Figure 7: MT measurement, configuration 2

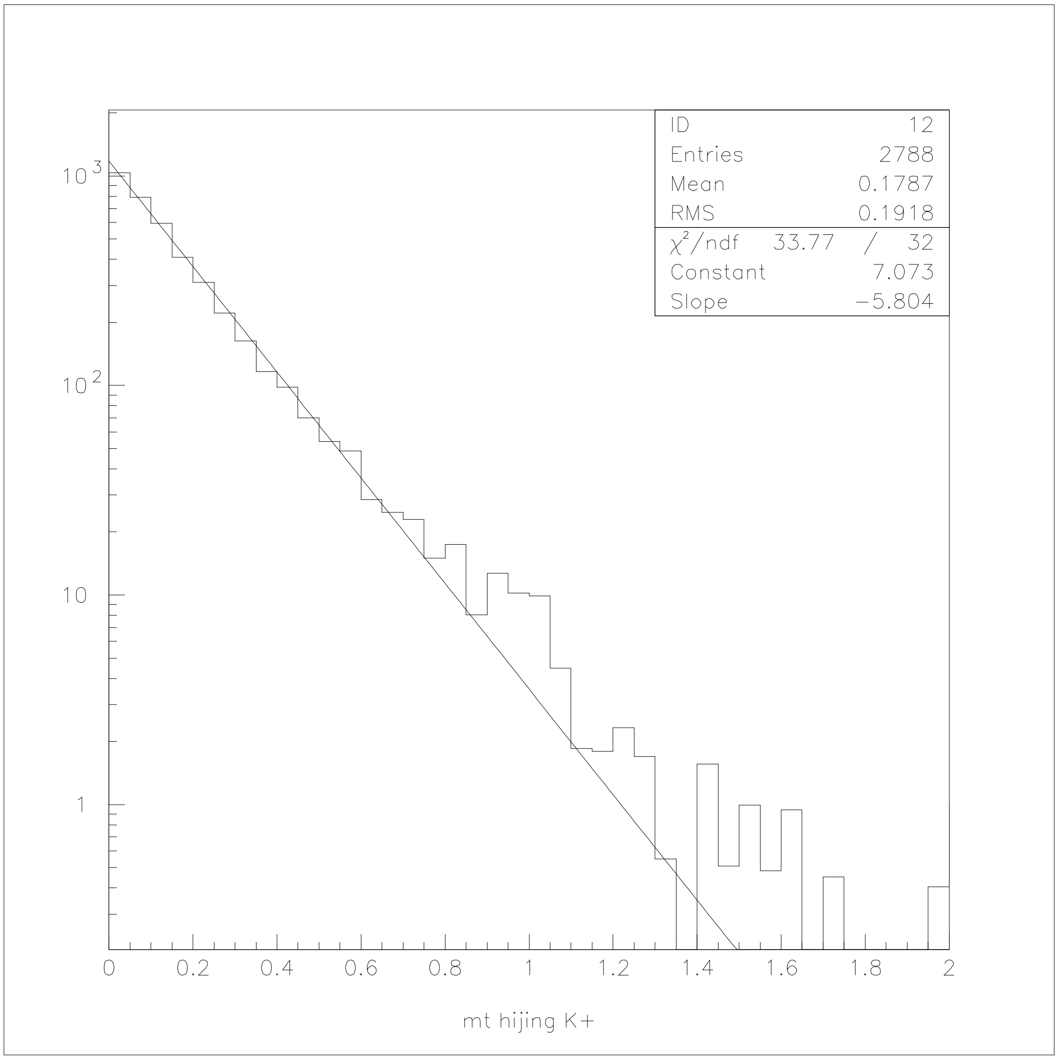

Figure 8: MT distribution for K+ in Hijing. The line is a fit with slope of 170 MeV

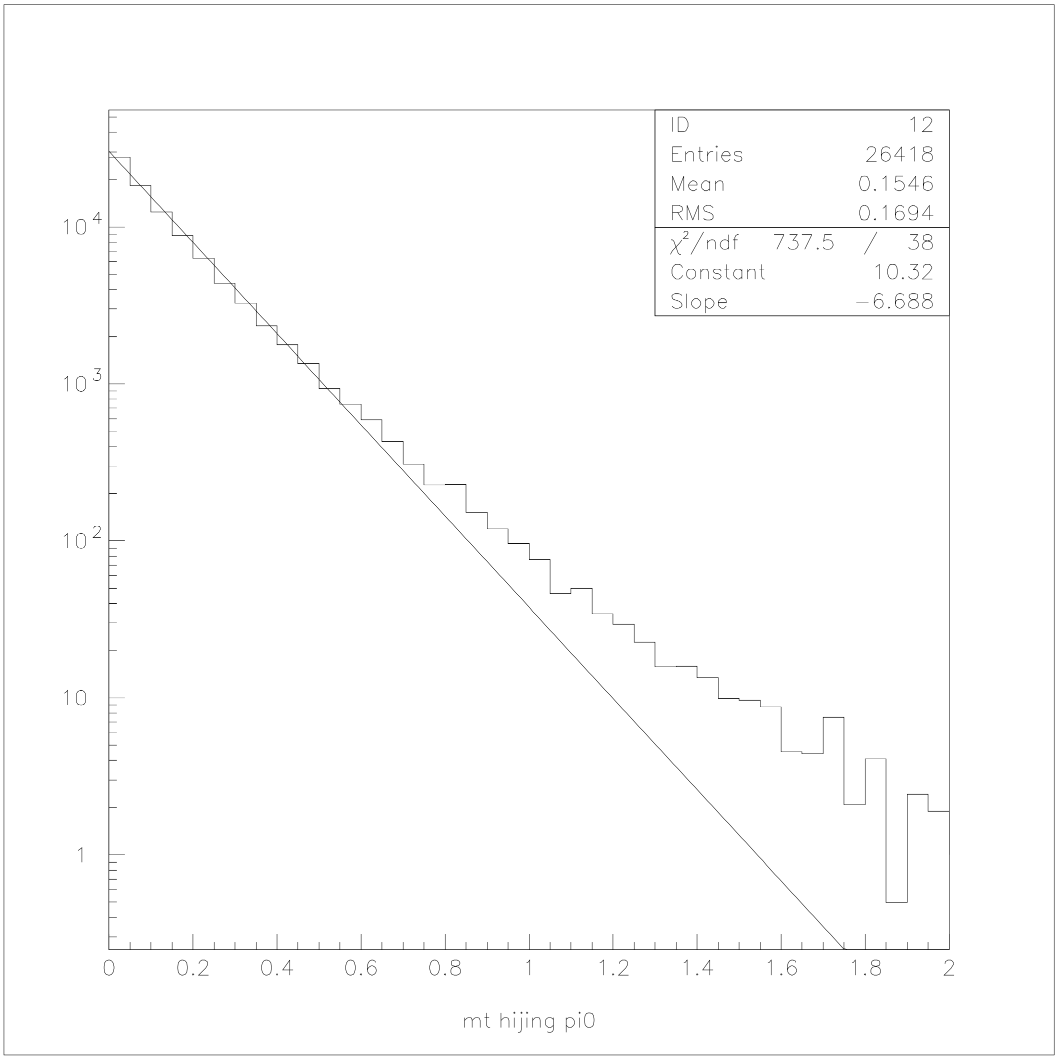

Figure 9: MT distribution for pi0 in Hijing. The line is a fit with slope 150 MeV

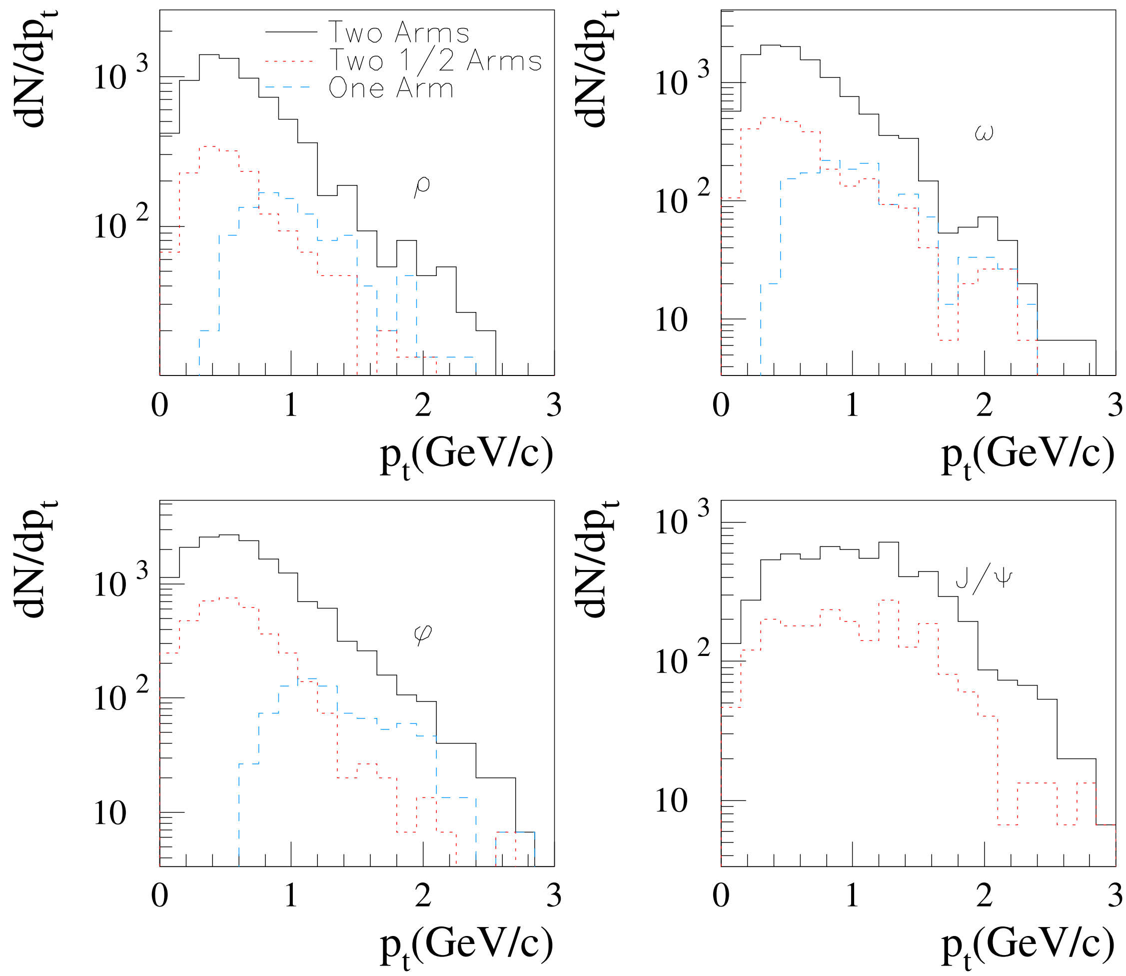

Figure 10: The transverse momentum distribution for ρ, ω, ϕ and J/ψ for central events after one year of running. The various lines correspond to the full PHENIX detector, two half-arms, and a single arm.

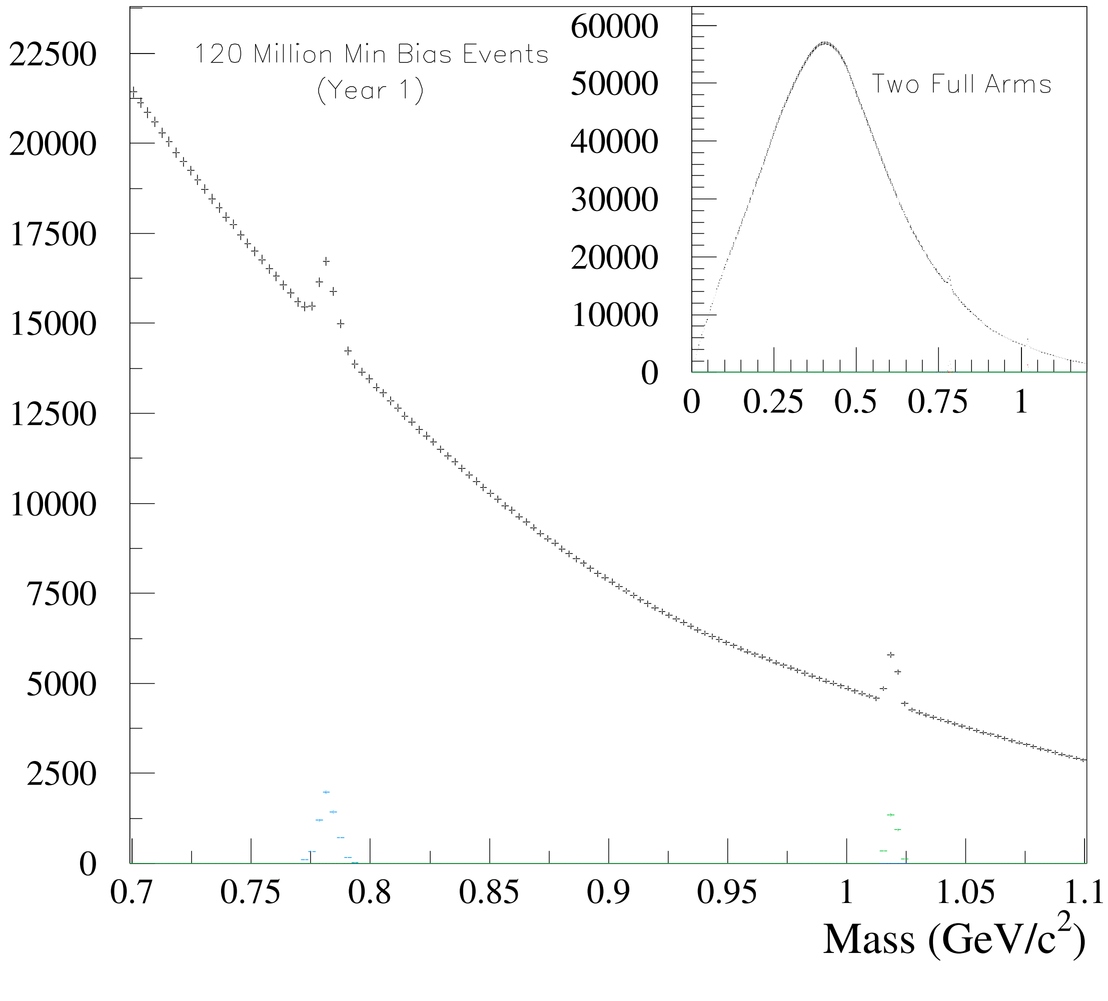

Figure 11: The invariant mass spectrum for the full PHENIX spectrometer after the first year of running. See the text for details.

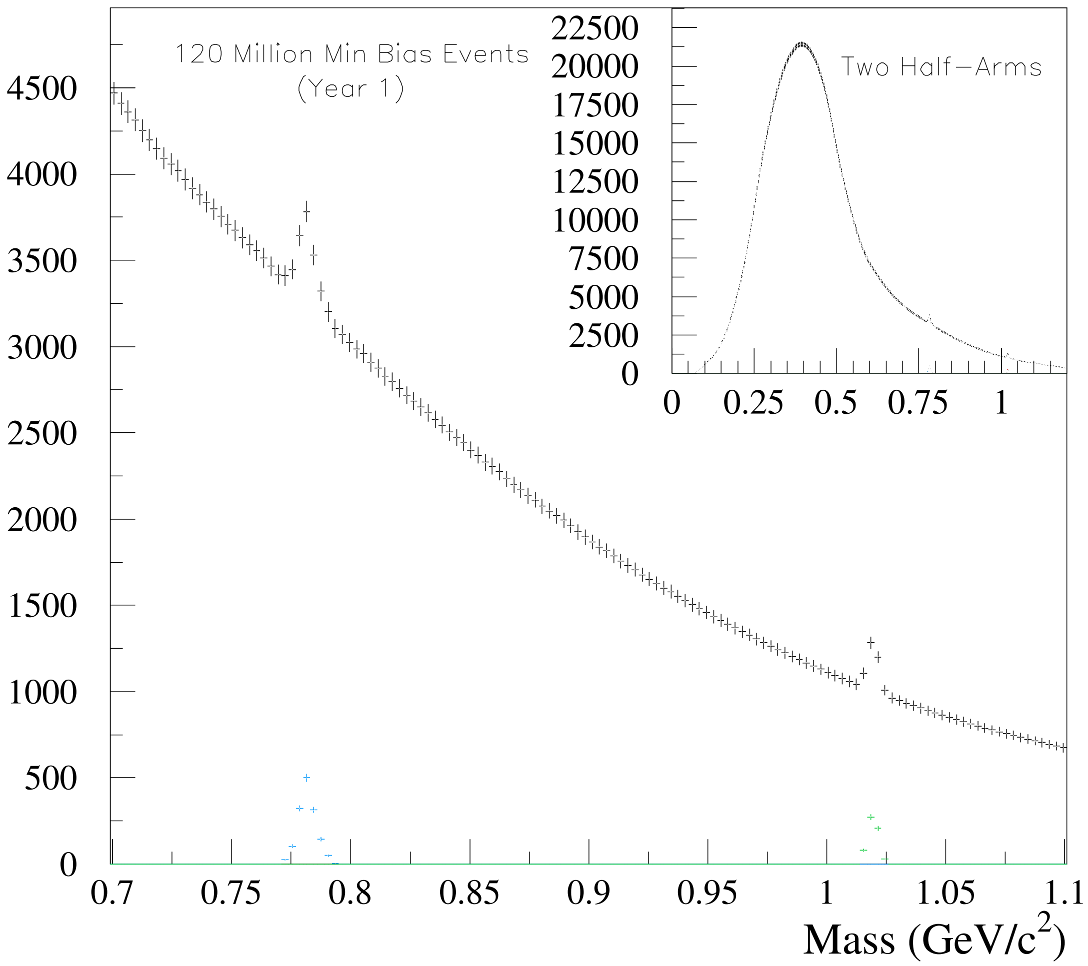

Figure 12: The invariant mass spectrum for 2 half-arms after the first year of running. See the text for details.